QUANTIFYING SCALING LAW FEATURES: OPEN DATA TO TACKLE INTERTWINED ENVIRONMENTAL AND SOCIAL CHALLENGES

Anna Carbone
Politecnico di Torino
https://www.polito.it/en/staff?p=anna.carbone

TED4LAT Workshop,
WIDERA, Horizon Europe Project
Valmiera, 14-18 July 2025

Urban Scaling Laws[1]

Aggregate urban features Y are linked to population size N by power-laws

$$Y \sim Y_0 N^{\beta} \tag{1}$$

where Y_0 is a normalization constant and β is a scaling exponent capturing the non-linearity of Y as a function of N.

$$\begin{cases} \beta > 1 & \text{Socio-economic features} \\ \beta \approx 1 & \text{Individual features} \\ \beta < 1 & \text{Infrastructures features} \end{cases} \tag{2}$$

[1] Luís MA Bettencourt et al. "Growth, innovation, scaling, and the pace of life in cities". In: *Proceedings of the National Academy of Sciences* 104.17 (2007), pp. 7301–7306.

Patents vs Population: Data for 107 Italian Metropolitan Areas 20 years[2]

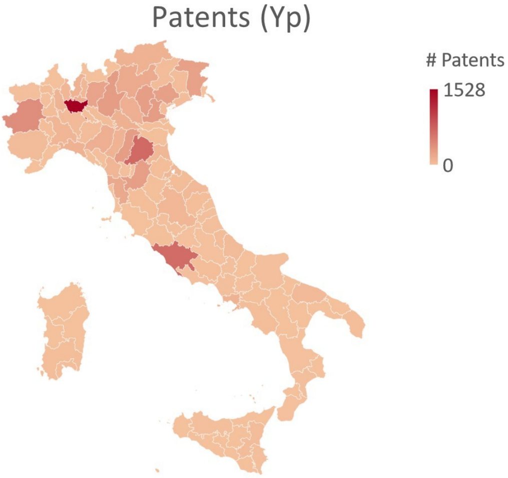

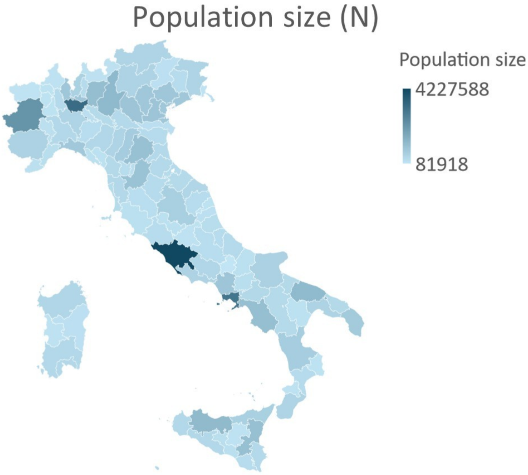

[2] Laura Alcamo et al. "A multi-scale approach to quantifying metropolitan innovation and recycling behaviour". In: *Journal of Infrastructure, Policy and Development* 8.9 (2024).

Recycled waste fractions vs Population: Data for 107 Italian Metropolitan Areas 20 years

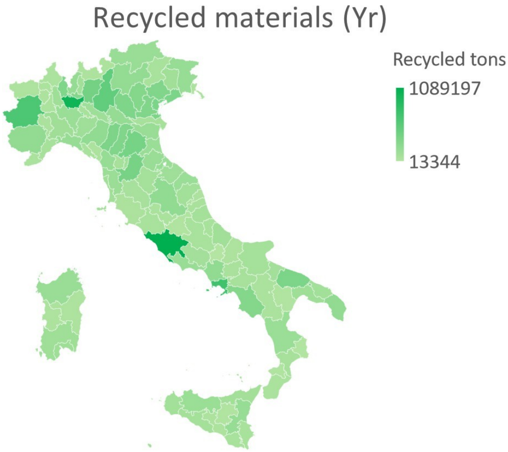

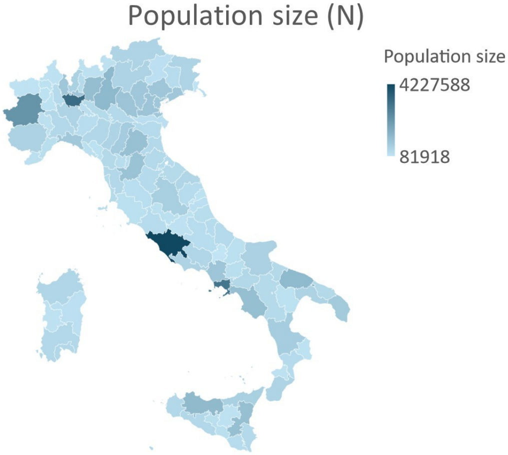

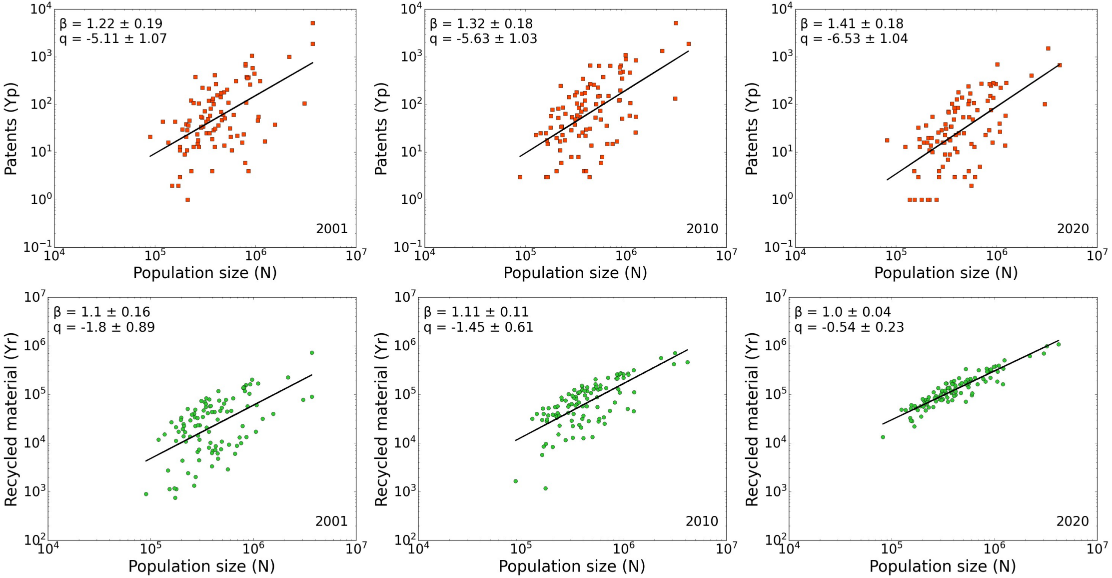

β = 1.22 ± 0.19
q = -5.11 ± 1.07
2001
β = 1.32 ± 0.18
q = -5.63 ± 1.03
2010
β = 1.41 ± 0.18
q = -6.53 ± 1.04
2020
Patents (Yp)
Population size (N)
β = 1.1 ± 0.16
q = -1.8 ± 0.89
2001
β = 1.11 ± 0.11
q = -1.45 ± 0.61
2010
β = 1.0 ± 0.04
q = -0.54 ± 0.23
2020
Recycled material (Yr)
Population size (N)

Year (1)	Patents' families (2)				Patents (3)				Recycled material (4)			
	$\beta \pm \Delta\beta$	R^2	R^2 Adj	ρ	$\beta \pm \Delta\beta$	R^2	R^2 Adj	ρ	$\beta \pm \Delta\beta$	R^2	R^2 Adj	ρ
2001	1.11 ± 0.15	0.37	0.36	0.73	1.22 ± 0.19	0.31	0.30	0.72	1.10 ± 0.16	0.32	0.31	0.66
2002	1.19 ± 0.18	0.32	0.31	0.69	1.38 ± 0.21	0.31	0.30	0.68	1.09 ± 0.14	0.33	0.32	0.67
2003	1.06 ± 0.17	0.31	0.31	0.69	1.11 ± 0.21	0.25	0.24	0.68	1.06 ± 0.14	0.32	0.31	0.71
2004	1.26 ± 0.15	0.42	0.41	0.74	1.36 ± 0.19	0.37	0.36	0.73	1.06 ± 0.13	0.33	0.32	0.74
2005	1.29 ± 0.16	0.40	0.40	0.74	1.47 ± 0.20	0.36	0.36	0.73	1.05 ± 0.12	0.40	0.39	0.76
2006	1.30 ± 0.14	0.47	0.47	0.73	1.50 ± 0.18	0.44	0.43	0.72	1.08 ± 0.12	0.42	0.41	0.76
2007	1.31 ± 0.15	0.46	0.45	0.74	1.40 ± 0.19	0.38	0.37	0.74	1.06 ± 0.12	0.41	0.40	0.77
2008	1.39 ± 0.14	0.49	0.49	0.76	1.57 ± 0.17	0.46	0.46	0.76	1.06 ± 0.11	0.44	0.43	0.79
2009	1.30 ± 0.15	0.44	0.44	0.74	1.35 ± 0.18	0.38	0.38	0.70	1.07 ± 0.11	0.49	0.49	0.84
2010	1.27 ± 0.15	0.43	0.42	0.72	1.32 ± 0.18	0.35	0.35	0.68	1.11 ± 0.11	0.52	0.51	0.83
2011	1.19 ± 0.16	0.36	0.35	0.69	1.25 ± 0.21	0.28	0.27	0.64	1.10 ± 0.10	0.57	0.56	0.87
2012	1.31 ± 0.18	0.36	0.35	0.67	1.56 ± 0.20	0.40	0.39	0.63	1.08 ± 0.09	0.57	0.57	0.88
2013	1.27 ± 0.15	0.44	0.43	0.67	1.42 ± 0.20	0.36	0.36	0.64	1.08 ± 0.09	0.64	0.64	0.91
2014	1.29 ± 0.18	0.35	0.34	0.66	1.42 ± 0.24	0.28	0.27	0.62	1.08 ± 0.09	0.60	0.60	0.91
2015	1.15 ± 0.16	0.36	0.36	0.66	1.25 ± 0.18	0.32	0.32	0.63	1.05 ± 0.08	0.64	0.64	0.92
2016	1.33 ± 0.16	0.42	0.41	0.65	1.38 ± 0.19	0.36	0.35	0.63	1.05 ± 0.07	0.65	0.65	0.93
2017	1.39 ± 0.16	0.45	0.44	0.67	1.48 ± 0.19	0.40	0.39	0.66	1.04 ± 0.06	0.73	0.73	0.94
2018	1.40 ± 0.17	0.41	0.41	0.71	1.39 ± 0.19	0.35	0.35	0.70	1.02 ± 0.05	0.80	0.80	0.95
2019	1.43 ± 0.16	0.45	0.45	0.71	1.43 ± 0.18	0.39	0.38	0.70	1.02 ± 0.04	0.83	0.82	0.95
2020	1.34 ± 0.15	0.45	0.44	0.73	1.41 ± 0.18	0.39	0.38	0.71	1.00 ± 0.04	0.85	0.85	0.95
2001-2020	1.41 ± 0.15	0.45	0.45	0.72	1.46 ± 0.17	0.41	0.41	0.69	1.04 ± 0.08	0.64	0.64	0.89

Microscopic origin of Urban Scaling Laws[3]

Infrastructural and socio-economic features are written as power laws of the population size $Y \sim N^{\beta}$ respectively with exponents:

$$\beta_i = 1 - \frac{D_f}{d(d + D_f)} \qquad \beta_s = 1 + \frac{D_f}{d(d + D_f)} \quad . \tag{3}$$

[3] Luís MA Bettencourt. "The origins of scaling in cities". In: *science* 340.6139 (2013), pp. 1438–1441.

Microscopic origin of Urban Scaling Laws[4]

The interaction strength between individuals is modelled in terms of a scalar field varying inversely with the distance, yielding power laws for the infrastructural and socio-economic quantities with scaling exponents respectively:

$$\beta_i = \frac{\gamma}{D_f} \qquad \beta_s = 2 - \frac{\gamma}{D_f} \quad , \tag{4}$$

with γ varying in the range $1.0 \div 1.5$ (noteworthy $\gamma = 1.0$ corresponds to the Newtonian gravitational law in $d = 2$).
The long-range interaction regime, with $\gamma / D_f < 1$, implies $\beta_s > 1$, i.e. that superlinear socio-economic scaling behaviour occurs when each individual can interact with all other individuals of the city.

[4] Fabiano L Ribeiro et al. "A model of urban scaling laws based on distance dependent interactions". In: *Royal Society open science* 4.3 (2017), p. 160926.

Microscopic origin of Urban Scaling Laws[5]

City buildings extend over three dimensions. Socio-economic interactions are assumed to occur in a three dimensional rather than in a two-dimensional fractal infrastructure . The population is distributed in a fractal space, with dimension D_p, where $D_f \leq D_p \leq D_f + 1$. The scaling exponents for the infrastructures and the socio-economic activities as:

$$\beta_i = \frac{D_f}{D_p} \qquad \beta_s = 2 - \frac{D_f}{D_p} \quad . \tag{5}$$

[5] Carlos Molinero and Stefan Thurner. "How the geometry of cities determines urban scaling laws". In: *Journal of the Royal Society interface* 18.176 (2021), p. 20200705.

Microscopic origin of Urban Scaling Laws[6]

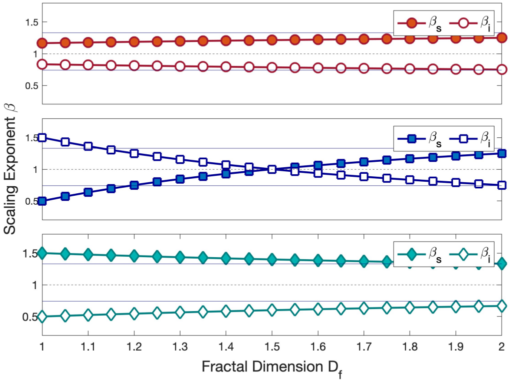

β_i	β_s
$1 - \frac{D_f}{d(d+D_f)}$	$1 + \frac{D_f}{d(d+D_f)}$
$\frac{\gamma}{D_f}$	$2 - \frac{\gamma}{D_f}$
$\frac{D_f}{D_p}$	$2 - \frac{D_f}{D_p}$

[6] Anna Carbone et al. "Atlas of urban scaling laws". In: *Journal of Physics: Complexity* 3.2 (2022), p. 025007.

earth.esa.int/eogateway/catalog/worldview-2-european-cities

→ THE EUROPEAN SPACE AGENCY

earth online • MISSIONS • DATA • TOOLS •

Data / WorldView-2 European Cities

WorldView-2 European Cities

Navigate To

- How to Access Data
- Available to Residents of the Following Countries
- Collection Description
- Technical Details
- Having Problems Accessing Data?
- Resources
- Discover Latest Data

DATA SET SPECIFICATIONS

Spatial coverage:	66 N, 26 S, 19 W, 35 E
Temporal coverage:	2010-07-20 - 2015-07-19
Date of launch:	2009-10-08
Operators:	Maxar
Mission status:	onGoing
Orbit height:	770 km
Orbit type:	Sun-synchronous
Swath width:	16.4 km
Resolution:	Very High Resolution - VHR (0 - 5m)
Wavelengths:	VIS (0.40 - 0.75 µm), NIR (0.75 - 1.30 µm)
Product types:	WV-110__2A

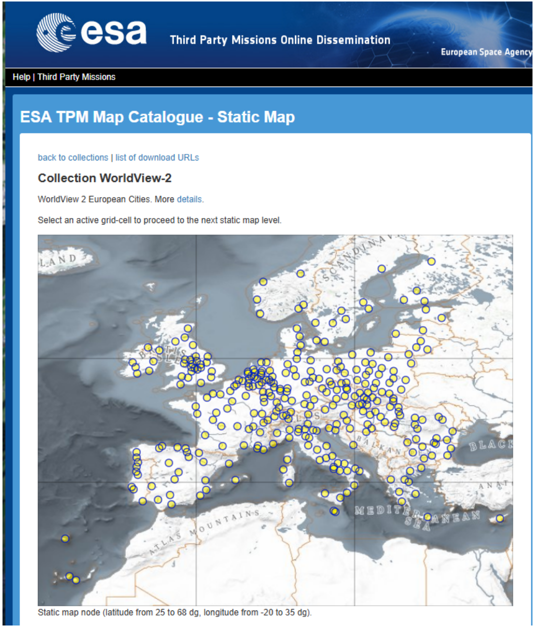

The WorldView Series consists of high resolution commercial Earth imaging satellites.

WorldView-1 (2007) world's first 50 cm resolution commercial imaging satellite

WorldView-2 (2009) the first high resolution 8-band multispectral commercial satellite.

WorldView-3 (2014) similar to WorldView-2 but positioned in a lower orbit

WorldView-4 (2016) 31 cm panchromatic imagery and 1.23 m multispectral imagery

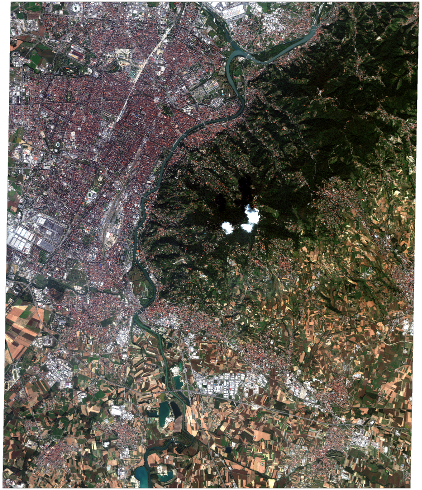

City: Torino

ID: N45-024

X: 45.024

Y: 7.709

Date: 09-2011

City: Zurich
ID: N47-377
X: 47.37
Y: 8.500
Date: 04-2014

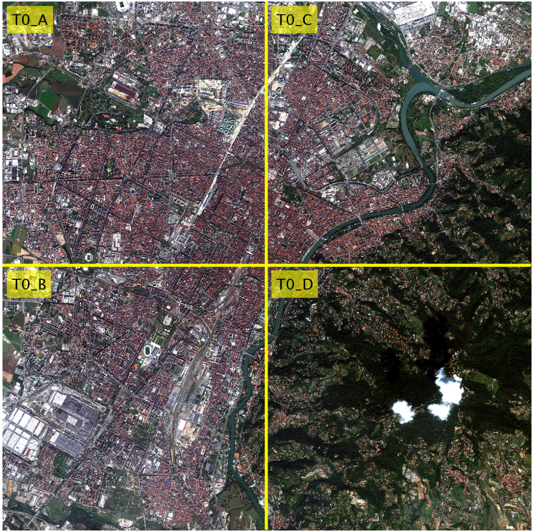
T0_A
T0_C
T0_B
T0_D

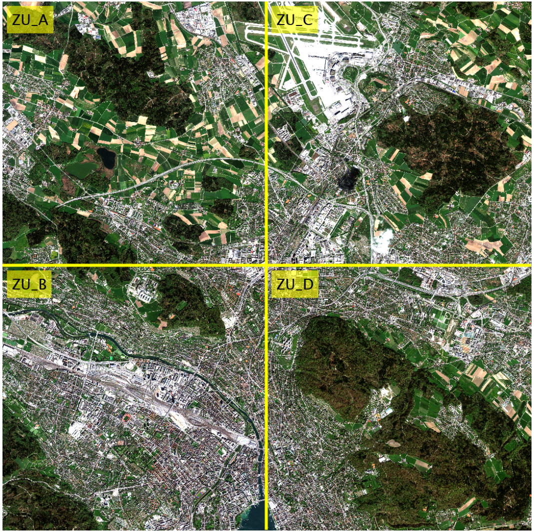
ZU_A
ZU_C
ZU_B
ZU_D

Detrending Moving Average algorithm for arbitrary-dimensional fractals[7]

The generalized variance $\sigma^2_{DMA}(s)$ is written as:

$$\sigma^2_{DMA}(s) = \frac{1}{V} \sum_V \left[f(r) - \widetilde{f}_{n_1,n_2,n_3}(r) \right]^2 , \tag{6}$$

where $f(r) = f(x_1, x_2, x_3)$ is the fractional Brownian field with $i_1 = 1, 2, ..., N$, $i_2 = 1, 2, ..., N$, $i_3 = 1, 2, ..., N$. The function $\widetilde{f}_{n_1,n_2,n_3}(x_1, x_2, x_3)$ is given by:

$$\widetilde{f}_{n_1,\, n_2,\, n_3}(r) = \frac{1}{\nu} \sum_{k_1} \sum_{k_2} \sum_{k_3} f(x_1 - k_1, x_2 - k_2, x_3 - k_3) , \tag{7}$$

with the size of the subcubes $(n_1,\ n_2,\ n_3)$ ranging from $(3, 3, 3)$ to the maximum values $(n_{1max},\ n_{2max},\ n_{3max})$. $\nu = n_1 n_2 n_3$ is the volume of the subcubes. The quantity $V = (N_1 - n_{1max}) \cdot (N_2 - n_{2max}) \cdot (N_3 - n_{3max})$ is the volume of the fractal cube over which the averages $\tilde{f}$ are defined.

[7] Anna Carbone. "Algorithm to estimate the Hurst exponent of high-dimensional fractals". In: *Physical Review E* 76.5 (2007), p. 056703.

Detrending Moving Average Algorithm for arbitrary-dimensional fractals

Fractal fileds with $H = 0.5$.

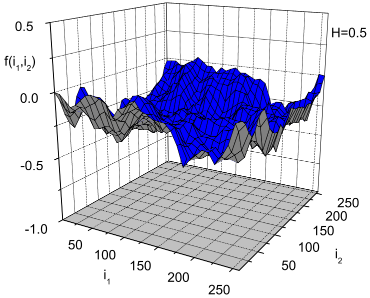

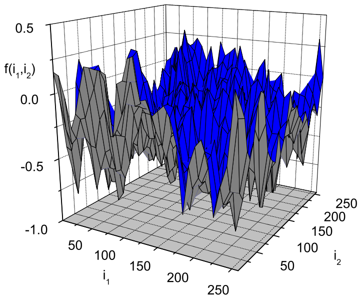

Detrending Moving Average Algorithm forfor arbitrary-dimensional fractals

Averaged Fractal fields with $H = 0.5$.

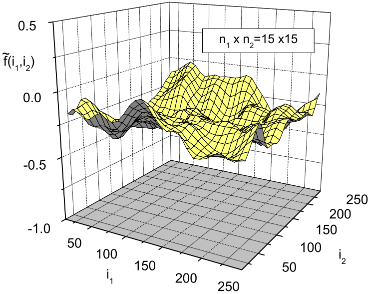

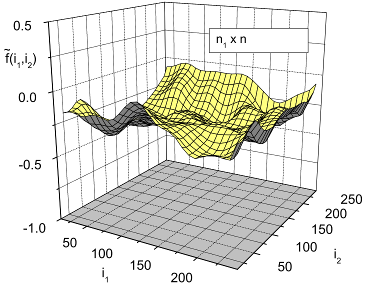

Detrending Moving Average Algorithm for arbitrary-dimensional fractals

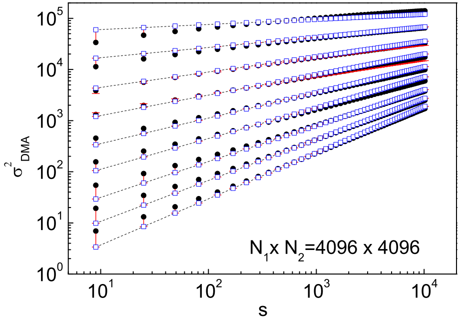

The plot of σ^2_{DMA} vs. $\mathcal{S} = \sqrt{(n_1^2 + n_2^2)}$ is a straight line, corresponding to the scaling relation:

$$\sigma^2_{DMA} \sim \left[\sqrt{(n_1^2 + n_2^2)}\right]^{2H}$$

$$\sigma^2_{DMA} \sim \mathcal{S}^{2H}$$

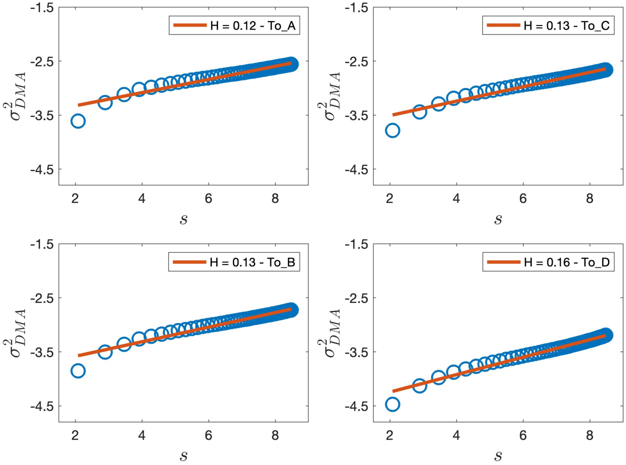

H = 0.12 - To_A
H = 0.13 - To_C
H = 0.13 - To_B
H = 0.16 - To_D
σ^2_{DMA}
s
-1.5
-2.5
-3.5
-4.5
2
4
6
8

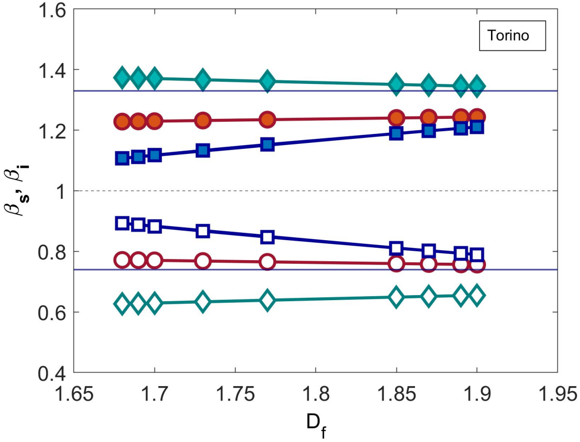

Torino
1.6
1.4
1.2
1
0.8
0.6
0.4
1.65
1.7
1.75
1.8
1.85
1.9
1.95
D_f
β_s, β_i

THANKS FOR YOUR ATTENTION !

Anna Carbone
Politecnico di Torino
email:anna.carbone@polito.it